Final Report: Planetary Entry System Synthesis Tool, A Method for Hypersonic Aerodynamic Shape Optimization

Guggenheim School of Aerospace Engineering
Georgia Institute of Technology
Atlanta, GA

Dr. Robert D. Braun
John E. Theisinger

March 31, 2008

Several different approaches to shape optimization are explored to identify hypersonic aeroshell shapes that will increase landed mass capability by maximizing drag-area for a specified lift-to-drag ratio. The most basic approach manipulates standard parameters associated with analytic aeroshell shapes like the sphere-cone and ellipsled. More general approaches manipulate the control points of a spline curve or surface. The parametric polynomial formulations of the Bezier and B-spline curves and surfaces are employed due to their desirable properties in shape design. Hypersonic aerodynamic analyses are carried out using Newtonian flow theory panel methods. An integrated optimization environment is created, and a variety of optimization methods are applied. In addition to a lift-to-drag ratio constraint, size constraints are imposed on the aeroshell, as determined by payload volume requirements and launch vehicle shroud size restrictions. Static stability and center-of-gravity placement required to achieve hypersonic trim are also considered during optimization. An example case is presented based on the aeroshell for the Mars Science Laboratory mission.

Nomenclature

B	=	Bernstein polynomial
$\mathbf{C}$	=	parametric curve Cartesian coordinate vector
C_DA	=	drag-area (= D/ q_∞)
C_LA	=	lift-area (= L/ q_∞)
C_m	=	pitching moment coefficient
C_mAl	=	pitching moment per unit free-stream dynamic pressure (= M/q_∞)
C_p	=	pressure coefficient
D	=	drag force or diameter
f	=	merit function
L/D	=	lift-to-drag-ratio
L	=	length or lift force
k, l, m, n	=	parametric polynomial degrees
m	=	mass
$\mathbf{n}$	=	unit surface normal vector
M	=	pitching moment
N	=	B-spline basis function
$\mathbf{P}$	=	control point Cartesian coordinate vector
q_∞	=	free-stream dynamic pressure
r_n	=	nose radius
$\mathbf{S}$	=	parametric surface Cartesian coordinate vector
t	=	knot parametric coordinate
u, w	=	curve or surface parametric coordinates
$\mathbf{V}_\infty$	=	free-stream velocity vector
w	=	width or objective weight
x, y, z	=	Cartesian coordinates
α	=	angle of attack
β	=	ballistic coefficient
θ	=	half-cone angle

I. Introduction

IN many entry, descent, and landing (EDL) missions, aeroshell shapes are designed to achieve a specified lift-to-drag ratio (L/D) with a maximum drag-area (C_DA). Such aeroshells take advantage of increased capabilities due to lift without sacrificing their ability to decelerate safely and effectively prior to terminal descent and landing. These aeroshell shapes can be determined using an integrated optimization environment which performs shape design based on computation of hypersonic aerodynamics.

Various methods of shape representation and manipulation exist, many born out of computer-aided geometric design (CAGD) theory. Parametric spline formulations have been shown to be very powerful for shape design and optimization since complex shapes can be generated with a relatively small number of control points or design variables. Selection of the appropriate shape representation and manipulation technique is critical for effective shape design and optimization.

II. Background and Motivation

Aeroshells are designed to deliver payloads safely through a planetary atmosphere, protecting the payload from the high aerodynamic heating and loads encountered during EDL. An aeroshell generally consists of a forebody which faces the flow and a backshell which completes the encapsulation of the payload. The specific shape of a particular aeroshell is driven by EDL performance requirements and thermal/structural limitations. Four different aeroshell shapes are shown in Fig. 1: the Viking-era 70° sphere-cone, the Mars Microprobe, the Aeroassist Flight Experiment (AFE), and a swept biconic design. This diversity in configurations is a direct result of differing mission and flight systems requirements – that is, form has followed function in every case.

Fig. 1 Various aeroshell shapes.[1, 2, 3, 4]

Fundamentally, C_DA represents the amount of drag force that an aeroshell is capable of generating at a given free-stream condition (D/q_∞). During the hypersonic EDL phase, this drag force provides the means to decelerate, implying that C_DA should be maximized for a given system mass (m). The ballistic coefficient is an aeroshell performance parameter that embodies this principle, relating inertial and drag forces as shown in Eqn 1.

$$\beta = \frac{m}{C_D A} \tag{1}$$

A higher β (high mass per unit drag-area) causes EDL events to occur at lower, denser portions of the atmosphere, reducing landed elevation capability and timeline margin. Additionally, peak dynamic pressure, heat rate, and integrated heat load are all higher, causing an increase in the thermal and structural loads that the entry system must be designed to accommodate.

Another important aeroshell performance parameter is the L/D of the aeroshell. A body of revolution, symmetric about its forward axis, will have an L/D of zero while flying at a 0° angle of attack (AOA or α). A body of revolution flying at a non-zero AOA, or an asymmetric body, however, can produce a non-zero L/D. Motivations for achieving a non-zero L/D aeroshell shape include:

- To relax the allowable approach navigation requirements (i.e., enabling a larger entry corridor).
- To reduce the deceleration loads.
- To mitigate atmospheric density and wind uncertainties.
- To improve landing accuracy.
- To increase parachute deployment altitude, enabling a higher surface elevation landing site or adding timeline margin.
- To execute a plane change or to provide a crossrange capability.

While a non-zero *L/D* has distinct advantages, care must be taken not to shape the aeroshell such that *L/D* is created at the expense of reducing C_DA and therefore increasing β. This risk can be seen more clearly in Eqn. 2 where *L/D* is written in terms of C_DA.

$$L/D = \frac{C_L A}{C_D A} \tag{2}$$

With these principles in mind, an ideal aeroshell shape would achieve a specified *L/D*, while maximizing C_DA and thereby minimizing β. This enables the aeroshell to perform as needed while sacrificing as little critical drag-area as possible – preserving its capability to deliver a payload to the planetary surface safely and effectively.

III. Methodology

This work is divided into three main components: hypersonic aerodynamic analysis, shape representation and manipulation, and shape optimization. The following sections detail each component and discuss how these components were integrated to create the capability to perform aeroshell shape optimization.

A. Hypersonic Aerodynamics

The Newtonian impact model for hypersonic flow allows aerodynamics to be determined from shape alone, independent of any flow parameters.[5] The coefficient of pressure (C_p) is computed based on the orientation of the surface, indicated by the unit surface normal vector (**n**), relative to the free-stream flow velocity ($\mathbf{V}_\infty$), as written in Eqn. 3.

$$C_p = 2\left(\frac{\mathbf{V}_\infty}{|\mathbf{V}_\infty|}\cdot\mathbf{n}\right)^2 \tag{3}$$

For a complex geometry, the entire body surface can be divided into panels and the C_p can be determined for each of these panels by knowing only their associated normal vector (see Eqn. 3). With the pressure distribution determined over the entire body, the forces and moments can be resolved through integration over the surface area.

Routines were coded in MATLAB to determine the aerodynamic parameters for a given shape. A matrix, containing the points that represent the aeroshell shape is input, along with AOA. Based on these inputs, a surface of panels is created. The vectors along the sides of the panels are used to determine the panel's normal vector using the cross product operation, and then the C_p for the panel is computed via Eqn. 3. Finally, the aerodynamic forces and moments are determined using the resulting pressure distribution and panel areas. Sideslip is not modeled; aeroshells are only allowed to vary in AOA. In order to maintain trim and stability outside of the AOA plane, aeroshells are required to be symmetric across the AOA plane, causing the rolling and yawing moments to be zero for all angles of attack.

In locating the center of gravity (CG) of the aeroshell, a uniform packaging density is assumed, which effectively places the CG at the volume centroid of the aeroshell. The CG offset required to trim an aeroshell is determined based on the computed forces and moments about this centroid. Because this CG offset is achieved by shifting the payload, it is generally best to keep the CG offset as small as possible to permit reasonable packaging configurations.

To be statically stable, an aeroshell must experience a restoring moment when disturbed from the trim AOA (i.e., $dC_m/d\alpha < 0$). Computationally, static stability is assessed using a finite difference calculation of the moments about the offset CG to calculate this derivative. To maximize static stability, this derivative must be as large a negative number as possible.

It should be noted that the scope of this study does not encompass aerothermodynamic considerations that also affect aeroshell design. This includes the blunting of the aeroshell nose and shoulder that would be required in order to reduce localized heating. Inviscid Newtonian flow theory is most appropriate in the design of blunt, hypersonic bodies, for which pressure drag dominates over viscous drag. Additionally, while modified Newtonian flow theory offers improvements in the accuracy of computed hypersonic aerodynamics for blunt bodies, the inclusion of $C_{P,\max}$ as parameter would simply scale the results uniformly, resulting in the same optimized shape with different absolute values for the aerodynamic parameters. Straight Newtonian theory ($C_{p,\max} = 2$) has thus been used here.

B. Shape Representation and Manipulation

1. *Analytic Shapes*

Analytic shapes offer the ability to define an aeroshell shape in terms of a few geometric parameters, reducing the number of design variables for optimization while allowing for smooth, manufacturable, and realistic shapes to be designed and analyzed. The main drawback to this approach is that aeroshell shapes are inherently restricted to a certain family, greatly limiting the variety and generality of possible designs. Two analytic shape families are explored in this work: the sphere-cone and the ellipsled.

The sphere-cone is parameterized in terms of four design variables: the nose radius (r_n), cone angle (θ), maximum diameter (D), and the AOA (α), as shown in Fig. 2. A representative sphere-cone aeroshell with its Newtonian pressure distribution is also shown in this figure.

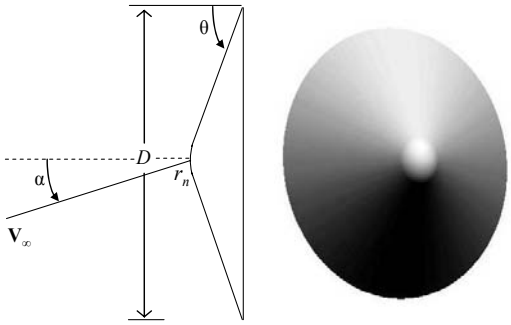

Fig. 2 Sphere-cone aeroshell shape.

The ellipsled is an analytic aeroshell shape composed of two half-ellipsoids with a cylindrical backshell. It is parameterized in terms of six design variables: the top nose radius ($r_{n,upper}$), bottom nose radius ($r_{n,lower}$), width (w), nose length (L_n), body length (L_{body}), and the AOA (α). These parameters are depicted in Fig. 3. A representative ellipsled aeroshell is also shown with the associated Newtonian pressure distribution in this figure.

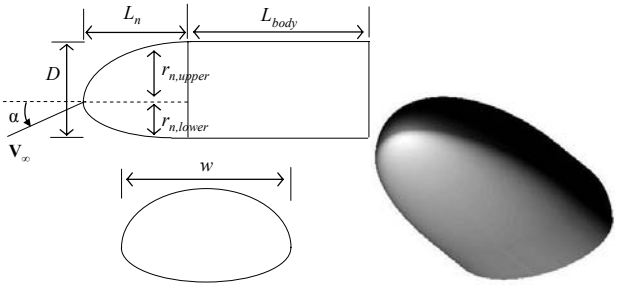

Fig. 3 Ellipsled aeroshell shape.

2. *Surfaces of Revolution*

To expand the range of possible shapes, forms with increasing levels of geometric control are implemented. The first improvement is to examine aeroshells represented as surfaces of revolution (SORs). An axial profile is first created from a series of control points, which then define a curve based on a chosen representation. That axial profile is rotated about the centerline to form an axisymmetric surface. While SORs can be used to represent analytic shapes that are axisymmetric, such as the sphere-cone, they also allow a broad range of other, non-analytic shapes. The limitation of the SOR approach is that all shapes generated are axisymmetric.

Each SOR representation generates an axial profile based on the positioning of control points. The control points, along with the AOA, are the design variables used for shape optimization. The control points can be allowed to vary with either one or two degrees of freedom (1-DOF or 2-DOF), dictating the number of design variables. For the 1-DOF case, the axial positions of the control points are fixed to a cross-section and the only DOF for each point is the radial direction. This arrangement is shown in Fig. 4.

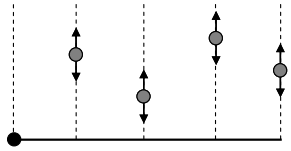

Fig. 4 1-DOF control point profile.

In the 2-DOF case, the control points are also allowed to vary axially, but only within defined bounds. This limited range of motion prevents control points from crossing and producing twisted shapes. The 2-DOF approach allows for a wider variety of axial profiles, increasing the size of the design space. This arrangement is shown in Fig. 5.

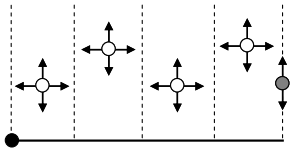

Fig. 5 2-DOF control point profile.

Note that as shown in these figures, either case requires a completely fixed point at the nose of the SOR and an axially-fixed point at the end of the SOR. This ensures the generation of a closed body with a specified length.

Once control points are positioned, a specific curve representation describes the SOR profile. Several different methods for curve representations were investigated: the direct-mesh, Bezier curve, and B-spline curve representations.

The most basic method for generating axial profiles is a direct-mesh approach. The profile is represented by a linear interpolation of the control points, as illustrated in Fig. 6.

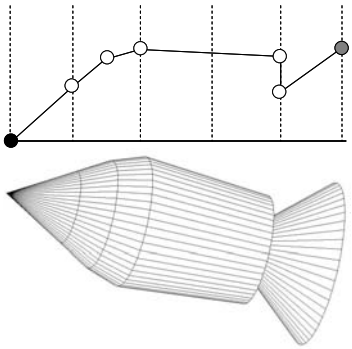

Fig. 6 2-DOF direct-mesh profile and SOR.

The direct-mesh SOR is an intuitive choice because the profile interpolates the control points. However, one disadvantage of this approach is that the linear interpolation does not result in smooth aeroshell profiles, which may be undesirable for shape design and optimization. In order to approximate a smooth profile, a large number of control points is needed, a circumstance which becomes computationally burdensome for optimization routines. This faceting along the profile is apparent in Fig. 6. In order to allow for smooth profiles, without adding a large number of control points, a more general curve representation is required.

To expand the options for representing aeroshell geometries, it is advantageous to model the axial profile using a curve form which is smooth and continuous. Additionally, it is preferable to use a profile which is described in the form of a function. The equations for curves can be expressed explicitly or implicitly, but the preferred representation for numerical computation is in the parametric form. A parametric curve is represented in vector form as in Eqn. 4.

$$\mathbf{C}(u) = \left[x(u)\ \ y(u)\ \ z(u)\right]^T \tag{4}$$

The parameter u is bounded by $u_{\min}$ and $u_{\max}$. Because they have the ability to represent bounded and closed curves, parametric curves avoid many of the problems associated with the explicit and implicit forms.

Bezier curves are one formulation of parametric curves that are defined by weighting the given control points with parametric basis functions.[6] The first and last control points are interpolated by the curve, while the intermediate points are approximated. Additionally, the ends of the Bezier curve are tangent to the first and last legs of the control polygon formed by the control points. A Bezier curve with (n+1) control points is defined by a polynomial of degree n, calculated using Eqn. 5.

$$\mathbf{C}(u) = \sum_{i=0}^{n} \mathbf{P}_i B_{i,n}(u) \tag{5}$$

Here, $0 \le u \le 1$, where $\mathbf{C}(u)$ is a point on the curve and $\mathbf{P}_i$ is the vector location of a control point. $B_{i,n}(u)$ are the n^{th}-degree Bernstein polynomials which serve as the blending functions that weight the influence of each control point. These basis functions are calculated using Eqn. 6.

$$B_{i,n}(u) = \frac{n!}{i!(n-i)!} u^i (1-u)^{n-i} \tag{6}$$

An advantage of using the Bezier formulation is the convex hull property, which ensures that the curve will lie entirely within the polygon created by the control points. Additionally, the variation-diminishing property dictates the maximum amount of curve oscillation within the convex hull. Given these two properties, the designer can readily predict the shape of a curve based on its control polygon.

Because the degree of a Bezier curve is directly linked to the number of control points, profiles with many control points require higher-order curves and become costly to evaluate. This trouble is avoided by creating composite curves from several lower-order curves. In this work, cubic Bezier curves were used to model the SORs since cubic curves offer a good degree of flexibility with low computational cost. In order to maintain continuity between two curves, the end control point of the first curve and the starting control point of the second curve must be coincident. Furthermore, to maintain a smooth transition, continuity of slope is required at this junction. This second condition requires that the coincident control vertex and the control points on either side be co-linear, as illustrated in Fig. 7 for a composite cubic Bezier curve profile. The SOR generated using this profile is also shown in Fig. 7.

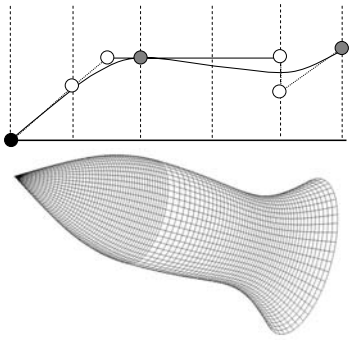

Fig. 7 2-DOF composite Bezier curve profile and SOR.

In terms of programming and manipulating continuous composite Bezier curves, the requirement of co-linear control points becomes tedious as the number of control points increases. Another limitation of the Bezier curve formulation is that changes to individual control points impact the entire curve (i.e., have global impact). To perform local shape design, it is helpful to employ a curve representation in which changes to an individual control point only influence a limited portion of the curve.

The B-spline is another parametric curve formulation which is actually a generalization of the Bezier curve formulation. As such, B-splines share the same desirable properties – particularly the convex-hull and variation-diminishing properties. The B-spline formulation is more complicated than the Bezier, with the introduction of knots, which essentially represent the parameter values at which composite curves connect. In order to maintain a closed-forebody aeroshell with a defined length, these knots can be fixed such that the first and last control points are interpolated and the curve is tangent to the first and last legs of the control polygon – similar to the Bezier formulation. This is achieved though multiplicity in knot values at the first and last control vertices.

Unlike the Bezier formulation, the degree of a B-spline curve is not strictly linked to the number of control points. However, the degree is limited by the number of control points as follows: (n+1) control points define a polynomial of degree (k-1), with (k-1) < (n+1). When k = (n+1), the B-spline formulation reduces to the Bezier formulation. The parametric equation for a B-spline is given by Eqn 7.

$$\mathbf{C}(u) = \sum_{i=0}^{n} \mathbf{P}_i N_{i,k}(u) \tag{7}$$

Here, $0 \le u \le u_{\max}$, and $N_{i,k}(u)$ are the B-spline basis functions, given by the recursive definition in Eqn. 8.

$$N_{i,k}(u) = (u - t_i)\frac{N_{i,k-1}(u)}{t_{i+k-1} - t_i} + (t_{i+k} - u)\frac{N_{i+1,k-1}(u)}{t_{i+k} - t_{i+1}} \tag{8}$$

$$\text{where: } N_{i,1} = \begin{cases} 1, & t_i \le u \le t_{i+1} \\ 0, & otherwise \end{cases}$$

The values of the knots, t_i, are stored in a knot vector. B-splines offer local control since they are essentially composed of composite curves, within which the control points are limited to influence. Additionally, continuity between composite curves is now automatic and no longer needs to be explicitly handled through the manipulation of control points. Specifically, cubic B-splines are curvature continuous.

3. Spline Surfaces

While the SOR representation of aeroshell geometries offers significantly more options for shape design than analytic shapes, all aeroshell shapes will be axisymmetric. In order to allow asymmetric aeroshell shapes (across the AOA plane), a general spline surface representation is required.

The parametric curve theory previously discussed is directly extensible to bi-parametric surface theory. Considering the advantages of the B-spline formulation noted when designing with parametric curves, a bi-parametric B-spline surface formulation was selected for implementation. These advantages include the fact that the number of control points is independent of the degree of the curve, and maintaining continuity does not require

explicit consideration of control point placement. These advantages apply in both parametric directions. A general bi-parametric surface is represented by Eqn 9.

$$\begin{aligned}\mathbf{S}(u,w) &= \left[x(u,w)\ \ y(u,w)\ \ z(u,w)\right]^T \\ &= \sum_{i=0}^{n}\sum_{j=0}^{m}\mathbf{P}_{ij}B_{i,k}(u)B_{j,l}(w)\end{aligned} \tag{9}$$

Here, $u_{\min} \le u \le u_{\max}$ and $w_{\min} \le w \le w_{\max}$. Analogous to the B-spline curve profile, the B-spline surface employed here is formulated to be clamped at its edges and has a uniform knot vector.

Shifting from a SOR to a B-spline surface formulation introduces several additional considerations. First, the control points defining the surface must each now be confined to a three-dimensional range of coordinates in order to prevent twisted shapes from being generated. This is a natural extension of the axial bounds placed on the control points used to generate axial profiles for the SORs. A cylindrical coordinate representation is used to position B-spline surface control points which extend radially from the apex of the aeroshell forebody to generate convex profiles. A B-spline surface is therefore generated by multiple, independently-defined axial profiles rather than a single profile as in the SOR case. The edge control points of the control mesh must also be confined to a single plane so that the generated aeroshell forebody will have a planar back-face. This planar back-face was generated naturally by the SOR representation. The cylindrical coordinate representation enables the size constraint of a circular envelope to be applied naturally as a side constraint (i.e., maximum radius) on control point radial positions. Thus, the constraint on aeroshell packaging within the launch vehicle shroud can easily be accommodated via the cylindrical coordinate representation. An arbitrary B-spline surface generated based on these constraints is shown in Fig. 8.

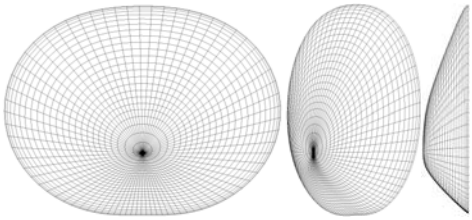

Fig. 8 B-spline surface front, oblique, and side views.

C. Optimization

Optimization was carried out using a variety of techniques. The objective of the optimization is to maximize the aeroshell C_DA while achieving a specified L/D. The design variables are the locations of the control points of the B-spline curve or surface and the AOA. The range of possible solutions is limited by dimensional and volumetric constraints. Additionally, terms that represent the CG offset and static stability are added to the objective function to minimize the CG offset required for static trim and maximize the static stability of the aeroshell.

A suitable optimization algorithm must be capable of exploring the large and complex design space that is likely to be highly nonlinear. Because aerodynamic analyses are rapid, a genetic algorithm (GA) is an ideal candidate optimizer for this problem. Genetic algorithms are in the family of zeroth-order optimization techniques in which the search for the optimum does not rely on the calculation of derivatives.

The main advantage of GAs is that they are able to find a global optimal solution for complex design space topologies with many local optima, while gradient-based methods may get stuck in any one of a number of local optima. Constraints are applied to GAs through the use of penalty functions. Penalties are applied to the fitness values for solutions lying outside of the feasible solution space. In this analysis, the feasible design space is defined by the geometric constraints of the aeroshell, including the size and volume limits, as well as the required hypersonic L/D. Side constraints are placed on the design variables to limit their ranges and obtain realistic aeroshell shapes from the spline curve and surface formulations.

Although GAs are capable of searching the entire solution space to find a global optimum, there are difficulties associated with determining the exact location of the maximum because genetic algorithms operate randomly and over a discretized design space. This problem can be solved as a hybrid optimization problem by pairing the GA with a gradient-based algorithm, such as the sequential quadratic programming (SQP) or method of feasible directions (MOFD) techniques. Gradient-based methods allow close convergence on a single-valued optimum solution.

The Phoenix Integration ModelCenter software is used to create the environment for aeroshell shape optimization. The built-in optimizer modules are used, along with MATLAB modules that were developed to perform shape generation and aerodynamic analyses. Once the parameters are defined for the optimization modules, and all input and output variables are appropriately linked, the hybrid optimizer can be executed. Due to the stochastic nature of the GA, multiple runs are performed in order to converge onto the optimum aeroshell shape.

IV. Validation

Validation of the tools within the optimization environment was performed by using shape optimization for a body with fixed length and volume. Based on supersonic slender body theory, the drag coefficient is independent of Mach number if the body has a pointed nose and ends in a cylindrical portion.[7] The drag is minimized if its area distribution, or profile, is that of a von Karman ogive. Given a base area and length, this profile can be determined. Comparison of a body optimized for minimum drag to the von Karman ogive quantifies the performance of the optimization environment.

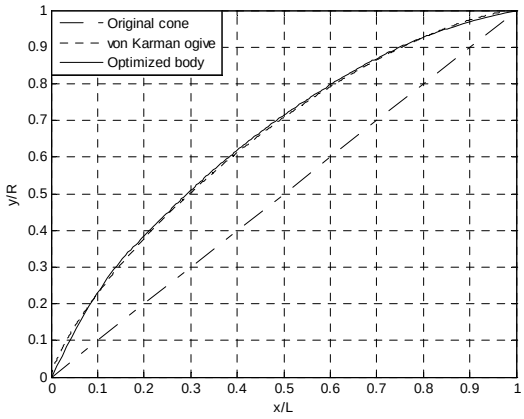

Fig. 9 Comparison of drag-minimized body profile to von Karman ogive profile.

The profile of a 15° sharp cone was generated using a B-spline curve. Starting with this profile, the optimizer was programmed to minimize C_DA, subject to a fixed volume and length, by varying the radial position of axially-fixed control points. The length and the base area of the optimized shape then uniquely defined an analytic von Karman ogive profile. The optimized profile is compared to the resulting von Karman ogive profile in Fig. 9, showing that the integrated optimization environment performed well by rapidly designing a B-spline profile that very closely matches the profile of the von Karman ogive.

V. Example Application

The Mars Science Laboratory (MSL) aeroshell was chosen as a baseline with which to explore the capabilities developed in this work. Packaging and EDL performance constraints were derived from published MSL geometry and mission requirements.[8]

An analytic, MSL-derived aeroshell is shown in Fig. 10 along with parameters computed from the hypersonic aerodynamic analysis. It has a 70° sphere-cone forebody with a conical backshell, designed to fly at a non-zero AOA, thereby producing an *L/D* of 0.24. There is a maximum-diameter constraint of 4.5 m dictated by the diameter of the launch vehicle fairing and the size of the integration and test facilities at the Jet Propulsion Laboratory. An equivalent aeroshell volume requirement of approximately 18 m^3 was determined from the present MSL design. A maximum-length constraint was determined based on the length of the MSL aeroshell, with a forebody length of approximately 0.75 m and a backshell length of approximately 2 m. Thus, an optimized aeroshell is required to fit within a 4.5-m diameter by 2.75-m high cylinder, have a volume of 18 m^3, and achieve an *L/D* of 0.24. All of these constraints are to be met while maximizing a multi-objective merit function comprised of a weighted sum of C_DA and terms to represent static stability and CG offset as shown in Eqn. 10.

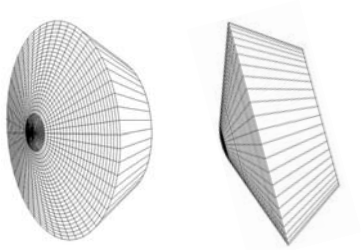

Parameter	Value
C_DA	25.56 m^2
CG offset	12.63 cm
$(C_mAl)_\alpha$	-12.75 m^3/rad
Merit, f	25.67

Fig. 10 Analytic approximation to the MSL aeroshell, α_{trim} = -15.5°.

$$f = w_1 \cdot C_D A - w_2 \cdot \left(C_m Al\right)_\alpha - w_3 \cdot \left|\text{CG offset}\right| \tag{10}$$

The w_i terms are the weights used to achieve a certain design objective. For this example, the weights were set equal for each term in the merit function, after each objective was scaled so that its contribution to the merit function was of the same order of magnitude. Two different shape representations were explored: cubic B-spline curve profiles to generate SORs and bi-cubic B-spline surfaces.

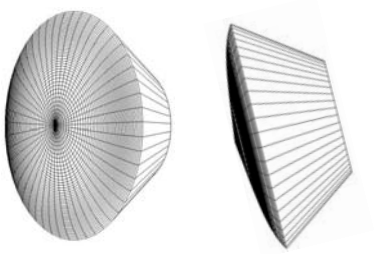

Parameter	% Change
C_DA	+4.70%
CG offset	-20.60%
$(C_mAl)_\alpha$	+12.90%
Merit, f	+8.46%

Fig. 11 B-spline SOR aeroshell, α_{trim} = -14.8°.

The cubic B-spline curve profile used here is defined by 15 geometric variables, which, including AOA, gives a total of 16 design variables for a given aeroshell shape. There are five 2-DOF control points and a sixth 1-DOF control point that defines the forebody-backshell interface. The aeroshell radius, forebody length, backshell length, and backshell angle are the other four geometric design variables. One resulting design is shown in Fig. 11.

This result highlights the fundamental trade between drag and stability in aeroshell shape design. The C_DA is slightly larger than that of the analytic aeroshell, due to an increase in bluntness of the forebody. However, this increase in drag-area comes at the expense of static stability (recall that to maximize static stability, this derivative must be as large a negative number as possible). An additional advantage of this non-analytic shape is that the required CG offset is smaller than that required for the analytic aeroshell since the blunter forebody produces smaller pitching moments.

In the treatment of bi-cubic B-spline surfaces, control point profiles are defined at equal angular intervals, radiating from an apex that is positioned vertically along the axis of symmetry. The resulting shape is symmetric across the AOA plane to prevent any rolling or yawing moments, but it is, in general, asymmetric across the horizontal plane. For radial profiles placed 45° apart with six control points along each profile, there are a total of 40 design variables after convexity constraints are taken into account. This tally of design variables also includes the AOA, backshell length, backshell angle, apex location, and forebody length. One resulting design is shown in Fig. 12.

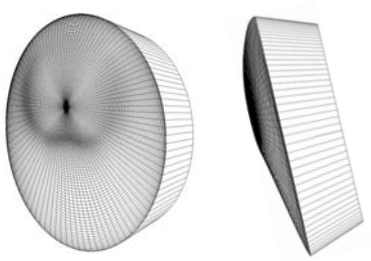

Parameter	% Change
C_DA	+3.15%
CG offset	-99.63%
$(C_mAl)_\alpha$	+12.31%
Merit, f	+46.08%

Fig. 12 B-spline surface aeroshell, α_{trim} = -13.6°.

Once again, the fundamental trade between drag and stability is evident as drag-area has been increased at the expense of static stability. While this aeroshell shows similar trends to that of the SOR aeroshell, the optimizer has exploited one capability of the asymmetric forebody. The forebody volume has been shifted off the centerline, enabling this aeroshell to achieve static trim with very little CG offset. Note that while the packaging volume has been kept constant, the "quality" of packaging volume should be considered here since this shallow backshell might prohibit certain internal payload configurations.

VI. Conclusions and Future Work

A capability to perform aeroshell shape optimization based on hypersonic aerodynamics has been developed. Several different methods for shape representation and manipulation have been investigated, including analytic and synthetic shapes. The possible geometry of analytic shapes is limited to certain families of shapes. The direct-mesh representation increases the flexibility of aeroshell designs but requires a large number of control points to approximate a smooth body. Synthetic, or spline, curve and surface formulations are used to improve modeling of the aeroshell shapes because they allow a large diversity of smooth-bodied shapes while maintaining a relatively low number of control points, or design variables, for optimization.

Two different types of synthetic curve formulations were considered: Bezier and B-spline. The B-spline formulation was found to be superior to the composite Bezier formulation. In order to maintain continuity between composite Bezier curves or surfaces, the coincident and adjacent control points are constrained to maintain certain spatial relationships. Maintaining these continuity conditions becomes cumbersome, but is automatic when using the B-spline formulation. The B-spline curve and surface formulations, while more complex in their underlying mathematics, are superior to the Bezier formulations because they do not explicitly require complex continuity constraints. This feature allows the aeroshell shape generation and analysis codes to be more flexible in optimization.

A hybrid optimization routine that combines a GA and a gradient-based algorithm was used to determine the optimal aeroshell shape. The combination of optimization algorithms improves the user's ability to avoid local optima by searching randomly over the entire design space. After deriving design constraints based on the MSL mission, aeroshell concepts were obtained that offer improved drag, stability and CG placement relative to the

analytic 70° sphere-cone which has been employed by all U.S. robotic Mars missions. The assessment of these aeroshell shapes also served to highlight the fundamental trade between drag and stability.

The natural progression for this work is to extend the options for shape representation and manipulation to rational spline forms, such as non-uniform rational B-spline (NURBS). This would enable the optimizer to explore quadric surfaces and conic profiles with an exact representation. Additionally, because Newtonian flow theory is only applicable to concave designs, clever methods need to be implemented to enforce strict concavity for the spline SOR and general spline surfaces. Due to the convex hull and variation-diminishing properties of these spline formulations, enforcing concavity can be achieved by generating a convex control polygon or mesh. Furthermore, the addition of aerothermodynamic constraints and considerations for packaging efficiency will add further design realism, while thermal protection system sizing and structural mass estimation will serve to assess the impact of aeroshell shape on total system mass. Various multi-objective and multi-disciplinary design optimization techniques will be applied to this problem to identify aeroshell configurations that are optimal from the stand-point of an overall EDL system and architecture.

References

[1] Braun, R. D. and Manning, R. M., "Mars Exploration Mars Exploration Entry, Descent and Landing Challenges," Paper 1076, 2006 IEEE Aerospace Conference, Big Sky, Montana, March 2006.

[2] Mitcheltree, R. A., DiFulvio, M., Horvath, T.J., and Braun, R. D., "Aerothermal Heating Predictions for Mars Microprobe," AIAA Paper No. 98-0170, Jan. 1998.

[3] Syvertson, C. A., "Research Problems in Atmosphere Entry and Landing for Manned Planetary Missions," NASA TN D-4977, Jan. 1969.

[4] Jones, J.J., "The Rationale for an Aeroassist Flight Experiment," AIAA Paper 87-1508, June 1987.

[5] Anderson, J.D., Hypersonic and High Temperature Gas Dynamics, AIAA Education Seris, AIAA, Reston, VA, 2000, pp. 46-50.

[6] Bartels, R. H., Beatty, J. C., and Barsky, B. A., An Introduction to Splines for Use in Computer Graphics and Geometric Modeling, Morgan Kaufmann Publishers, Inc., San Mateo, CA, 1987, pp. 25-45, 46-63, 211-213.

[7] Ashley, H. and Landahl, M., Aerodynamic of Wings and Bodies, Addison-Wesley, Reading ,MA, 1965.

[8] Edquist, K. T., Dyakonov A. A., Wright, and M. J., Tang, C. Y., "Aerothermodynamic Environments Definition for the Mars Science Laboratory Entry Capsule," AIAA Paper No. 2007-1206, Jan., 2007.